(2) The production of resonances in a large fraction of the events. The Δ^{++} isobar and the ρ and ω^0 mesons are important components in these final states just as they are in three- and four-body final states. The relative importance of the production of these resonances does not diminish with increasing pion multiplicity.

We report some evidence for the production of higher-mass resonances. Our results are not conclusive and require a more detailed experiment. Nevertheless, the general features that we have extracted from the data indicate that resonance production processes may be the major contributors at this energy to six- and seven-particle final states.

ACKNOWLEDGMENTS

We would like to express our gratitude to our scanning and measuring staff and to Argonne National Laboratory, the Zero Gradient Synchrotron (ZGS) operating staff, and the 30-in. bubble-chamber staff for their aid during this exposure. We are indebted to Dr. J. P. Chandler for computer programs used in the data analysis.

PHYSICAL REVIEW D VOLUME 1, NUMBER 1 1 JANUARY 1970

Properties of ${}_{\Lambda}H^{3}$†

G. KEYES
Argonne National Laboratory, Argonne, Illinois 60439 and Northwestern University, Evanston, Illinois 60201
AND
M. DERRICK, T. FIELDS,* AND L. G. HYMAN
Argonne National Laboratory, Argonne, Illinois 60439
AND
J. G. FETKOVICH, J. MCKENZIE, B. RILEY, AND I.-T. WANG
Carnegie-Mellon University, Pittsburgh, Pennsylvania 15213
(Received 29 September 1969)

The properties of the hypernucleus ${}_{\Lambda}H^{3}$ were measured in an analysis of helium-bubble-chamber pictures taken at the Argonne ZGS. Some 90 examples of the production reaction $K^{-}+He^{4}\rightarrow {}_{\Lambda}H^{3}+p+\pi^{-}$ were found in which the K^{-} stopped and the ${}_{\Lambda}H^{3}$ decayed via π^{-} emission. Twenty-seven events were observed to decay via the two-body mode ${}_{\Lambda}H^{3}\rightarrow \pi^{-}He^{3}$, with the remaining events decaying to $\pi^{-}pd$ or $\pi^{-}ppn$. The production rate was measured to be $(1.8_{-0.6}^{+0.7})\times10^{-3}$ per stopping K^{-}. The mean life of the hyperfragment was measured from the two-body decay mode as $(2.64_{-0.52}^{+0.84})\times10^{-10}$ sec. The lifetime obtained from the three-body decays was consistent with this value, after the elimination of a serious source of background. The binding energy of ${}_{\Lambda}H^{3}$ was measured to be 0.25 ± 0.31 MeV. The decay ratio $R_3=\Gamma({}_{\Lambda}H^{3}\rightarrow \pi^{-}He^{3})/\Gamma({}_{\Lambda}H^{3}\rightarrow \text{all } \pi^{-})$ was measured to be $0.36_{-0.06}^{+0.08}$, in agreement with values from previous experiments and with the value calculated for spin $\frac{1}{2}$ for the ${}_{\Lambda}H^{3}$ hypernucleus.

I. INTRODUCTION

THE properties of the Λ-N interaction can be studied experimentally either by the scattering of free Λ hyperons or by measurements of the properties of hypernuclei. Since the low-energy scattering is dominated by the triplet interaction, and the spins of the S-shell hypernuclei ${}_{\Lambda}H^{3}$, ${}_{\Lambda}H^{4}$, and ${}_{\Lambda}He^{4}$ show that the singlet interaction is dominant in the ground state, these two types of experiment are somewhat complementary. The lightest hypernucleus known, ${}_{\Lambda}H^{3}$, consists of a Λ particle weakly bound to a deuteron core and so gives a system that should be most amenable to theoretical understanding.

The Λ-N phenomenology, developed particularly by Dalitz and his co-workers,[1] predicts the lifetimes and decay branching ratios of the light hypernuclei ${}_{\Lambda}H^{3}$, ${}_{\Lambda}H^{4}$, ${}_{\Lambda}He^{4}$, and ${}_{\Lambda}He^{5}$. The calculations together with the existing data provide a self-consistent phenomenological account of the properties of the S-shell systems.[2] In particular, the model correctly accounts for the π^{-}-to-π^{0} decay branching ratio of these hypernuclei and the lifetime of ${}_{\Lambda}H^{4}$. The decay rate of ${}_{\Lambda}H^{3}$ is predicted[3] to be $1.07\Gamma_{\Lambda}$ for $J=\frac{1}{2}$, corresponding to a lifetime of 2.35×10^{-10} sec. For several years the most accurate measurement of this lifetime was that carried out in a small helium bubble chamber.[4] The value obtained,

† Work supported by the U. S. Atomic Energy Commission.
* Also at Northwestern University, Evanston, Illinois 60201.
[1] R. H. Dalitz, *Nuclear Interactions of the Hyperons* (Oxford University Press, London, 1965).
[2] D. H. Davis and J. Sacton, in *High-Energy Physics*, edited by E. H. S. Burhop (Academic Press Inc., New York, 1967), Vol. II, p. 365.
[3] R. H. Dalitz, in *Proceedings of International School of Physics "Enrico Fermi," Course XXXVIII* (Academic Press Inc., New York, 1967), p. 89.
[4] M. M. Block, R. Gessaroli, S. Ratti, M. Schneeberger, L. Grimellini, T. Kikuchi, L. Lendinari, L. Monari, W. Becker, and E. Harth, in *Proceedings of the Sienna Conference on Elementary Particles and High-Energy Physics, 1963*, edited by G. Bernardini and G. P. Puppi (Società Italiana de Fisica, Bologna, 1963), p. 62.

$(0.95_{-0.15}^{+0.19})\times10^{-10}$ sec, is in serious disagreement with the calculation.

The present experiment[5] was designed to remeasure the properties of the $_{\Lambda}H^{3}$ hypernucleus—in particular, the lifetime—using a larger helium bubble chamber. The larger size and the magnetic field of 41 kG provide significantly better kinematic measurements than were previously obtained.

II. EXPERIMENTAL EQUIPMENT

A. Beam

The exposure was carried out at the Argonne ZGS in the 28° low-momentum separated beam. The beam, a conventional design with two stages of electrostatic separation, is shown in Fig. 1.[6] Low-momentum particles coming from a copper target placed in the ZGS were bent by 20° in the ZGS guide magnet and emerged through horizontal and vertical collimators CL 1 and CL 2 that defined the solid-angle acceptance of the beam. The first quadrupole doublet focused the beam horizontally at the first mass slit MS 1 and made the beam parallel in the vertical plane. The momentum selection was provided by the first bending magnet B 1 and was defined by the horizontal opening in the first mass slit. The vertical focus at the first slit was provided by Q 3. In the second stage all the vertical focusing was provided by the fringe field focusing in B 2, which bent the beam by 40°. The final double focus was made at the second mass slit by the last quadrupole doublet Q 5 and Q 6, as shown by the ray traces of Fig. 2.

Yield measurements made in the beam together with calculations of interactions and scattering in the degrader showed that an optimum transport momentum to provide stopping kaons in the chamber was 650 MeV/c. The highest K^{-} yield from the target was found at a production angle of about 8°. This larger yield of low-energy particles at nonzero angles was subsequently observed in other yield measurements.[7] The momentum bite was set nominally at $\pm1\%$, and 15 to 20 K^{-} mesons were obtained at the second mass slit for an average ZGS intensity of 4.3×10^{11} protons per pulse. The particles were degraded by a 9-cm Be plug located just outside the vacuum vessel and 11 cm of Cu sandwiched between the magnet coils. The median plane gap in the magnet was only 1.2 cm wide, so that a large fraction of the particles were scattered into the magnet coils and consequently failed to stop in the liquid helium. On the average, three kaons traversed the chamber per pulse, with one coming to rest in the liquid.

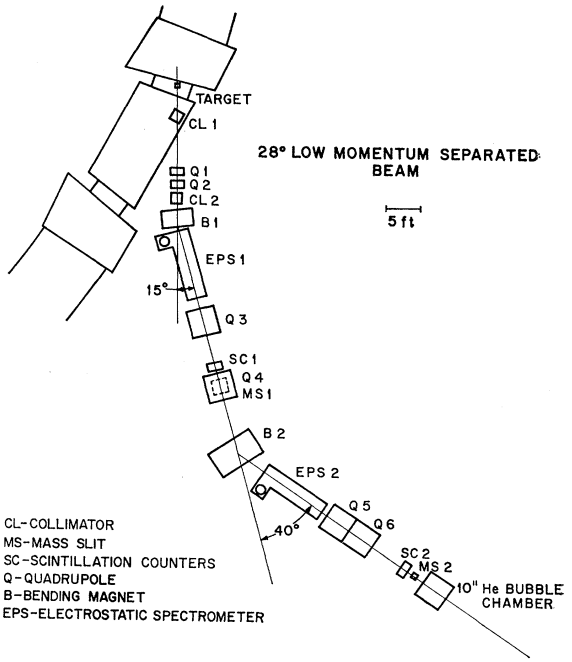

FIG. 1. Layout of the low-momentum separated beam in the 28° channel at the Argonne ZGS.

B. Bubble Chamber

The bubble chamber used in this experiment[8] was a cylinder 25 cm in diameter and 35 cm deep containing 18 liters of liquid helium. Expansions were made by a 2-mm movement of the plastic lens which was connected to the chamber body by a stainless-steel omega bellows, as can be seen in Fig. 3. Liquid helium from a reservoir was circulated through a heat exchanger at the top of the chamber to control temperature. Vapor-pressure thermometers located at the top and bottom of the chamber measured the temperature during the run to be 3.2°K, with a gradient from top to bottom of 0.05°K. Expansions were made every 2 sec to synchronize with the ZGS repetition rate, and a flash delay of 1.2 msec after the beam spill was used to allow the bubbles to grow to about 250 μ in diameter. The tracks were photographed on 35-mm film by three cameras mounted on a 25-cm-diam circle.

The optical constants of the chamber were determined in the usual way, by surveying the chamber fiducial system under the operating conditions as well as at room temperature. The relative positions of the chamber fiducials were accurately measured on the chamber

[5] For more experimental details see G. S. Keyes, Ph.D. thesis, Northwestern University, 1969 (unpublished). Preliminary results on the $_{\Lambda}H^{3}$ lifetime have been previously published: G. Keyes, M. Derrick, T. Fields, L. G. Hyman, J. G. Fetkovich, J. McKenzie, and I.-T. Wang, Phys. Rev. Letters **20**, 819 (1968).

[6] M. Derrick and G. S. Keyes, in Proceedings of the 1966 International Conference on Instrumentation for High-Energy Physics, 1966, p. 618 (unpublished).

[7] G. Marmer, K. Reibel, D. M. Schwartz, A. Stevens, T. A. Romanowski, C. J. Rush, P. R. Phillips, E. C. Swallow, R. Winston, and D. Wolfe, Phys. Rev. **179**, 1294 (1969); J. D. Davies, J. D. Dowell, P. M. Hatterslay, R. J. Homer, A. W. O'Dell, M. E. Sproul, A. A. Carter, K. F. Riley, R. J. Taper, D. V. Bugg, D. C. Slater, and E. J. N. Wilson, Nuovo Cimento **54**, 608 (1968).

[8] M. Derrick, T. Fields, L. Hyman, J. Loken, K. Martin, E. G. Pewitt, J. Fetkovich, and J. McKenzie, in Proceedings of the 1966 International Conference on Instrumentation for High-Energy Physics, 1966, p. 264 (unpublished).

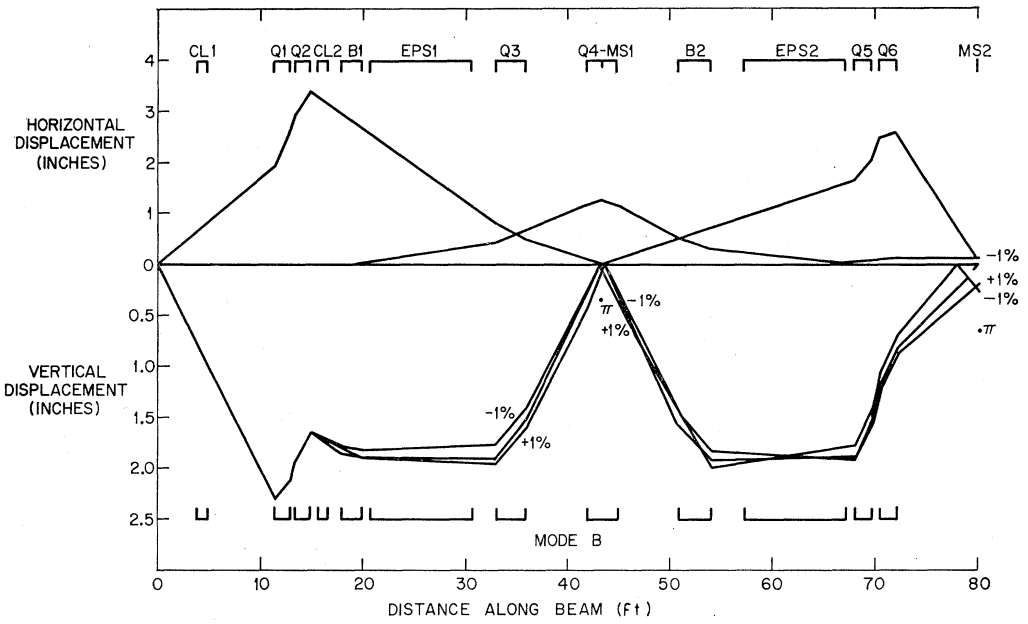

FIG. 2. Optical profiles for the 28° beam showing rays with the maximum divergence transported by the system. Trajectories for the design momentum $p_0=650$ MeV/c and $\pm 1\%$ p_0 are shown. The $K^-\pi$ separation using 450 kV across a 4-in. gap is indicated at the first and second foci.

glass at room temperature using a measuring microscope. Film measurements of the fiducial images together with the survey information were then used to reconstruct the camera positions and film plane tilts. This procedure gave a set of optical constants that allowed reconstruction of points in the chamber to an absolute accuracy of 30 μ in the xy plane normal to the optic axis and 180 μ in z.

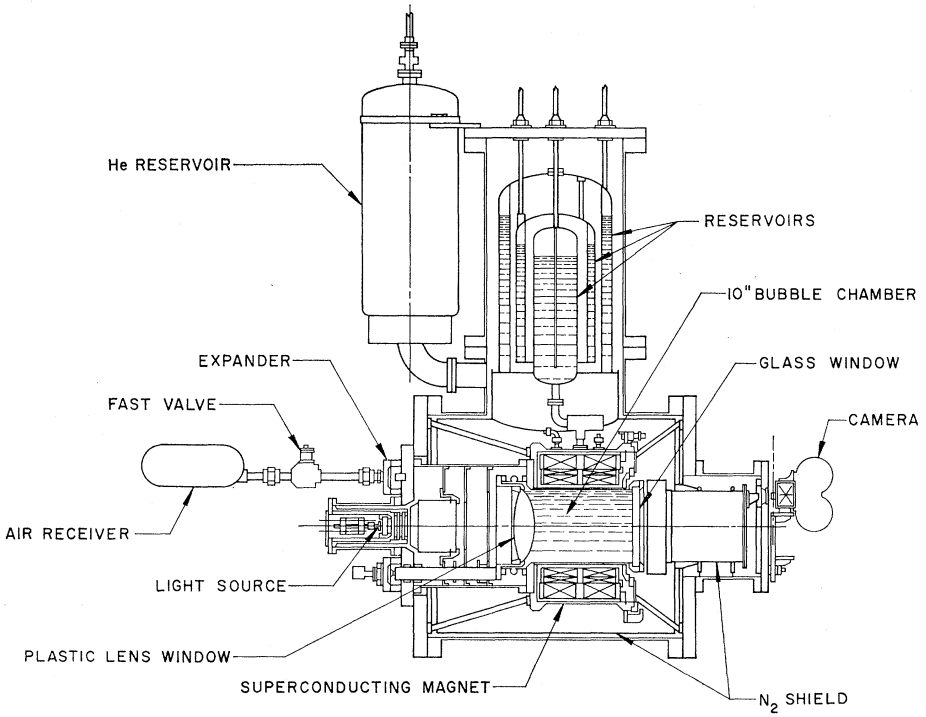

FIG. 3. Schematic diagram of the Argonne-Carnegie 25-cm superconducting-magnet helium bubble chamber used for this experiment.

The magnet assembly consisted of three concentric solenoids wound of NbZr and NbTi cabled superconductor.[9] The coils were charged in 19 h to a field of 41 kG. The time stability of the magnetic field was better than $\pm 0.1\%$ during the entire exposure. Since no ferromagnetic material was used, the magnetic field shape was simply calculated from the coil geometry. The field was also measured after the exposure using both a rotating coil and a flip coil.

The absolute value of the magnetic field was also determined by measuring the curvature of the decay track from the $K_{\pi 2}$ and $K_{\mu 2}$ decays of stopped K^{+} mesons, as well as from the τ decay mode of K^{+} and K^{-} mesons. Those decay pions that came to rest in the chamber had their momentum determined from range. A third check of the magnetic field was obtained by measuring a sample of 200 stopping pion tracks and comparing the momentum from range with the curvature information. The weighted mean of the determination using τ decays and stopping pion tracks gave a central field value of 40.94 ± 0.04 kG.

The density of helium in the chamber of 0.1390 ± 0.0004 g cm^{-3} was determined from the measured pressure and temperature at the operating conditions. The range-energy relation was then calibrated using the measured ranges of tritons (from the reaction $\pi^{-}+\mathrm{He}^{4} \rightarrow n+\mathrm{H}^{3}$) and the $_{\Lambda}H^{4}$ hyperfragments (from the reaction $K^{-}+\mathrm{He}^{4} \rightarrow {}_{\Lambda}\mathrm{H}^{4}+\pi^{0}$). The latter reaction, in which the hyperfragment has an equivalent proton energy of 2.02 MeV, provides a suitable starting point for integration of the Bethe-Bloch equation, while the measured triton range was used to deduce a mean ionization potential of 42.5 ± 0.8 eV.[10]

III. EXPOSURE AND ANALYSIS

During the exposure a total of 480 000 pictures were obtained, of which 275 000 were taken with a stopping K^{-} beam. This paper gives the results from a scan of 161 200 of these stopping K^{-} pictures.

The helium bubble chamber is a powerful tool for studying the $_{\Lambda}H^{3}$ lifetime since events can be selected that are kinematically overdetermined at both production and decay. The production reaction studied is

$$K^{-}+\mathrm{He}^{4} \rightarrow {}_{\Lambda}\mathrm{H}^{3}+p+\pi^{-}, \tag{1a}$$

followed by the possible π^{-} decay modes

$$_{\Lambda}\mathrm{H}^{3} \rightarrow \pi^{-}+\mathrm{He}^{3} \tag{1b}$$

$$\rightarrow \pi^{-}+d+p \tag{1c}$$

$$\rightarrow \pi^{-}+p+p+n. \tag{1d}$$

In general, the hyperfragment track is short, with a mean length of 5 mm, so it was necessary to scan the film carefully in order to avoid missing early decays that would bias the lifetime to longer values. The maximum $_{\Lambda}H^{3}$ range is over 4 cm, so care was also taken to avoid biases against long hyperfragment tracks which would lead to a systematic shortening of the measured lifetime.

IV. SCANNING

Scanning was done within a restricted fiducial volume that excluded regions of the chamber that were poorly illuminated or overexposed. The criteria called for a linear scan in two views where each beam track was followed across the fiducial volume or to an interaction vertex. All events with two associated negative pions, excluding obvious Λ decays, were selected so that even "zero-length" $_{\Lambda}H^{3}$ events should have been found. With these rules, approximately 100 event candidates per roll of 3100 frames were selected by the scanners. In addition to the hyperfragments, background events which could meet these criteria are

$$K^{-} \rightarrow \pi^{-}+\pi^{-}+\pi^{+}, \tag{2a}$$

$$K^{-}+\mathrm{He}^{4} \rightarrow \Lambda+\pi^{-}+p+d, \quad \Lambda \rightarrow \pi^{-}+p \tag{2b}$$

$$K^{-}+\mathrm{He}^{4} \rightarrow {}_{\Lambda}\mathrm{He}^{4}+\pi^{-}, \quad {}_{\Lambda}\mathrm{He}^{4} \rightarrow \pi^{-}+pppn \tag{2c}$$

$$K^{-}+\mathrm{He}^{4} \rightarrow \Sigma^{-}+\pi^{0}+ppn, \quad \Sigma^{-} \rightarrow \pi^{-}+n \tag{2d}$$

with $\pi^{0}+n \rightarrow \pi^{-}+p$.

All candidate events were edited by a physicist, and only those which satisfied more restrictive rules were passed on for measuring. The editing rules called for a positive prong or stub and a negative pion at production, and a negative pion with possibly one or two positive prongs or stubs at decay. Hyperfragment candidates which could be ambiguous with free Λ events, where the Λ decayed in spatial coincidence with either the beam track or a positive prong, were carefully scrutinized in all three views. If the Λ decay vertex could be clearly resolved from the overlying tracks, the event was rejected. If a Λ overlay was suspected but not obvious, a comment was recorded and the event was measured. Events with obvious Dalitz pairs at either production or decay were rejected by the editor. About 15% of the events selected by the scanners were actually classified as $_{\Lambda}H^{3}$ candidates by the editor.

The events reported on in this paper come from a scan of 52 rolls of film. Of this, 22 rolls were double-scanned at Argonne. The scanning efficiency on an individual scan of this film was $(85 \pm 15)\%$, resulting in a combined efficiency from both scans of $(98_{-10}^{+2})\%$. At Carnegie 30 rolls were scanned: 3 rolls once, 16 rolls twice, and 11 rolls three times. Of these 30 rolls, 13 were also scanned at Argonne (including the 3 rolls scanned only once by Carnegie). For the 17 rolls scanned only by

[9] C. Laverick and G. Lobell, Rev. Sci. Instr. **36**, 825 (1965).
[10] L. G. Hyman, J. Loken, E. G. Pewitt, M. Derrick, T. Fields, J. McKenzie, I.-T. Wang, J. Fetkovich, and G. Keyes, Phys. Letters **25B**, 376 (1967); and (unpublished).

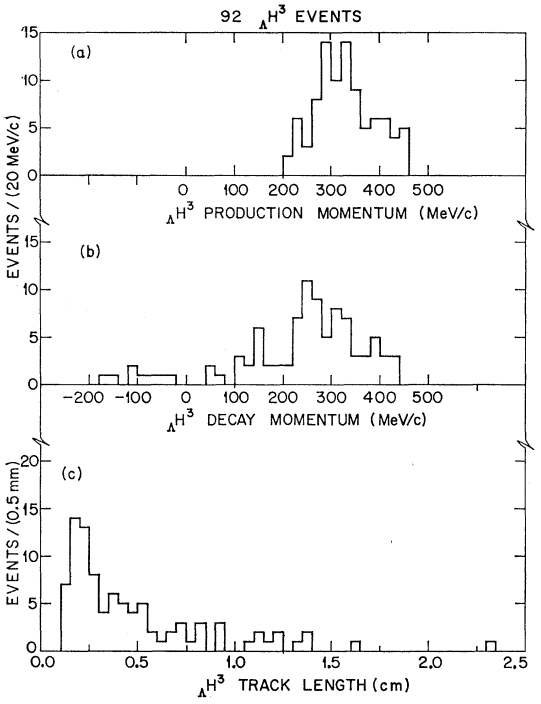

FIG. 4. Distributions for 92 kinematically fitted $_{\Lambda}H^3$ events from the production reaction $K^-+He^4 \rightarrow {}_{\Lambda}H^3+p+\pi^-$ followed by the decay $_{\Lambda}H^3 \rightarrow \pi^-+ppn$. The events shown have $_{\Lambda}H^3$ track length ≥ 1 mm, $_{\Lambda}H^3$ dip angle $\leq 65°$, incident K^- momentum consistent with zero, and χ^2 probability $\geq 1\%$ for a multivertex fit. (a) $_{\Lambda}H^3$ momentum at the production vertex; (b) $_{\Lambda}H^3$ momentum at the decay vertex; (c) $_{\Lambda}H^3$ track length.

Carnegie, the scanning efficiency on an individual scan was $(54\pm11)\%$, resulting in an estimated over-all efficiency for these rolls of $(74\pm14)\%$. The common 13 rolls were compared for scanning efficiency with respect to institution, and the Argonne and Carnegie efficiencies measured this way were equal, at $(77\pm21)\%$, giving a combined efficiency of $(94_{-9}^{+6})\%$. The over-all scanning efficiency for this experiment averaged $(88\pm9)\%$.

All the results given in this paper were calculated independently for the events found on only one scan, and in all cases were found to be consistent with the results obtained from the complete sample.

V. MEASURING AND COMPUTING

The events selected by the editing physicist as potential $_{\Lambda}H^3$ candidates were measured on standard manual measuring machines. The tracks were reconstructed in space by the geometry program TVGP and the events were fitted using a kinematic fitting program.[11] The error assignments of the geometry variables were checked both by measuring some events many times and by stretch plots, and found to be reasonable.

TABLE I. Topological distribution of $_{\Lambda}H^3$ events.

	π^-He^3	π^-pd	π^-ppn	Total
One-prong	19	6		25
Two-prong	8	23	0	31
Three-prong	0	35	1	36
Total	27	65		92

After the first measurements, candidates were classified into the following categories: (a) unambiguous, multivertex-fitted $_{\Lambda}H^3$ events, (b) Λ decays in coincidence with the incident K^- track, (c) $_{\Lambda}H^3$ multivertex fits ambiguous with $\Lambda\pi^-pd$ production where the Λ decays in spatial coincidence with the deuteron (these are called "Λ overlays"), (d) $_{\Lambda}He^4 \rightarrow \pi^-p$ He^3 events, (e) K^- interactions in flight, and (f) events giving no kinematic fits.

The only truly unambiguous $_{\Lambda}H^3$ events are those with just a visible negative pion at decay, and two-body decays in flight where the He^3 prong is visible. Decays into the three- or four-body final states with two or three visible prongs are nearly always kinematically ambiguous with events from reaction (2b), although the two-prong decays must be considered "second-order" accidents since the Λ decay vertex must then overlap not only the deuteron track but also its end point. The two-pronged decays were therefore initially accepted as legitimate $_{\Lambda}H^3$ events if the fit to the hyperfragment hypothesis had an acceptable confidence level. All of the candidates with three prongs at decay were reexamined on the scanning table under high magnification in an attempt to resolve any Λ overlay events whether or not they gave good $_{\Lambda}H^3$ fits. The no-fit events were also checked for scatters in any of the tracks or peculiarities that could require a special measuring procedure. All events were remeasured until each candidate was identified by three compatible results or until it became obvious that some pathological feature made the event unmeasurable.

In making the final selection of $_{\Lambda}H^3$ events for the lifetime determination, the following criteria were applied: (a) $_{\Lambda}H^3$ measured track length ≥ 1 mm, (b) $_{\Lambda}H^3$ dip angle $\leq 65°$, (c) momentum of incident K^- consistent with zero, (d) χ^2 probability $\geq 1\%$ for multivertex fit except for cases where only a production fit was possible (three-body one-prong decays and four-body two-prong decays), and (e) at least three compatible measurements and kinematic fits for each event. Details of the acceptable events are given in Table I. The momentum spectra of the $_{\Lambda}H^3$ at production and decay and the $_{\Lambda}H^3$ length distribution are shown in Fig. 4.

VI. LIFETIME ANALYSIS

The lifetime analysis was done using the maximum-likelihood technique. Each event was assigned a decay probability, and the likelihood function corresponding to the mean lifetime τ is then just the joint probability

[11] At Carnegie SQUAW was used for kinematic fitting, whereas at Argonne the local version of the CERN program GRIND was used.

for all events, written as

$$L(\tau)=\prod_{i=1}^{P}\frac{e^{-t_i/\tau}}{e^{-t_{0i}/\tau}}\prod_{j=1}^{Q}\frac{1}{\tau}\frac{e^{-t_j/\tau}}{e^{-t_{0j}/\tau}}\prod_{k=1}^{R}\frac{1}{\tau}\frac{e^{-t_k/\tau}}{e^{-t_{0k}/\tau}-e^{-T_k/\tau}}, \quad (3)$$

where t_i, t_j, and t_k are the observed flight times for P particles which decay at rest, Q which decay in flight with potential time less than some maximum T_j, and R which decay in flight with potential time greater than the maximum T_k. The time t_0 is the flight time required to attain the minimum accepted decay prong length, which was chosen as 1 mm. The $_{\Lambda}H^{3}$ was considered to decay at rest if its momentum at decay was less than 170 MeV/c (corresponding to a residual range of $\sim$1 mm), so the flight time t_i for these events was counted only to this point. The selection of 170 MeV/c as the cutoff momentum for in-flight decays was guided by Fig. 4(b), which reflects the measuring errors on the hyperfragment length and production momentum. This limit was set at a level which makes negligible the possibility of misclassifying true decays at rest as decays in flight, since a weighting factor of τ^{-1} is applied to the latter probability in the likelihood function. The decay time for each event was obtained from the calculated flight time for $_{\Lambda}H^{3}$ in helium using the range-energy relation measured in this chamber.

The lifetime can also be calculated using only events that decay in flight, in which case the likelihood function takes the form

$$L(\tau)=\prod_{i=1}^{R}\frac{1}{\tau}\frac{e^{-t_i/\tau}}{e^{-t_{0i}/\tau}-e^{-T_i/\tau}}, \quad (4)$$

where all symbols have the same meaning as before, except T_i, which is the smaller of the moderation time or the maximum acceptable potential time. The solutions of Eqs. (3) and (4) for the most probable value of the mean lifetime τ led to transcendental equations that were solved numerically.

The lifetime and errors were independently calculated using the Bartlett S function, with results that agreed well with those calculated by direct integration of the likelihood functions.

VII. RESULTS

A. Lifetime

The mean life calculated from the 27 two-body decays [reaction (1b)] is $(2.64_{-0.52}^{+0.84})\times10^{-10}$ sec, with the likelihood function shown in Fig. 5. The two-body decays

TABLE II. $_{\Lambda}H^{3}$ mean-lifetime results from this experiment.

	Two-body decays	Three-body decays
Argonne	$(2.64_{-0.64}^{+1.22})\times10^{-10}$ sec, 16 events	$(1.70_{-0.32}^{+0.51})\times10^{-10}$ sec, 27 events
Carnegie	$(2.64_{-0.72}^{+1.60})\times10^{-10}$ sec, 11 events	$(1.13_{-0.17}^{+0.24})\times10^{-10}$ sec, 38 events

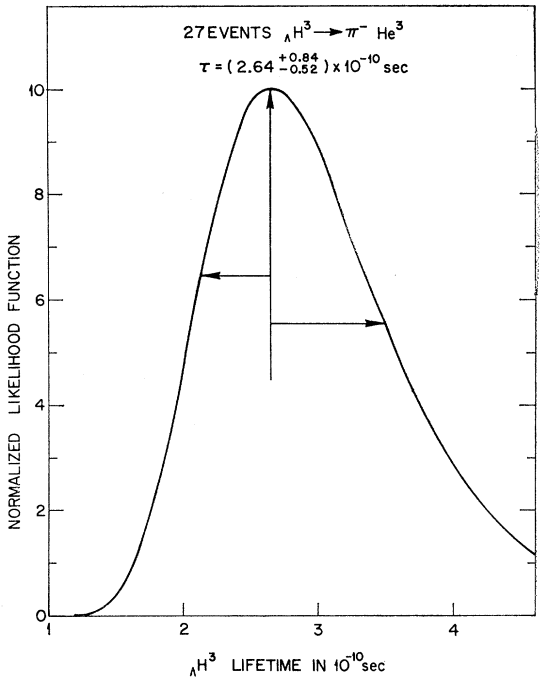

FIG. 5. Lifetime likelihood function for 27 $_{\Lambda}H^{3}$ events decaying into the two-body final state π^{-}He^{3}. The errors are calculated from the Bartlett S function described in Ref. 5.

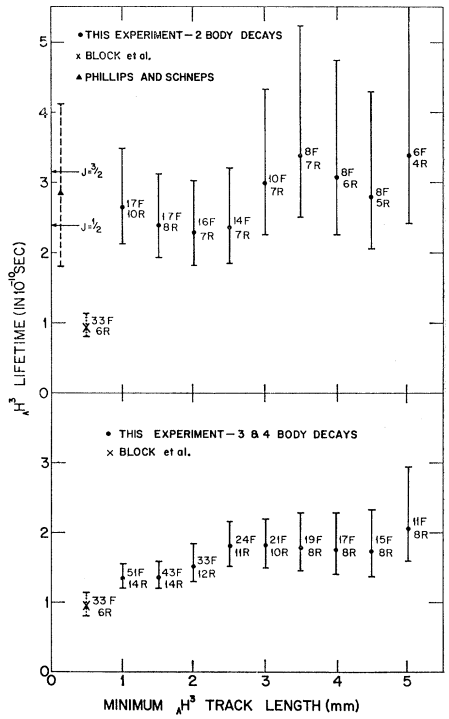

FIG. 6. $_{\Lambda}H^{3}$ lifetime results from this experiment for two-body and multibody decays as a function of the minimum accepted $_{\Lambda}H^{3}$ track length. The number of events that decayed in flight (F) and at rest (R) for each length cut are indicated. The measurements of Block *et al.* (Ref. 4) and Phillips and Schneps (Ref. 15) are shown, as well as the predicted lifetimes for both possible $_{\Lambda}H^{3}$ spin states, $J=\frac{1}{2}$ and $J=\frac{3}{2}$.

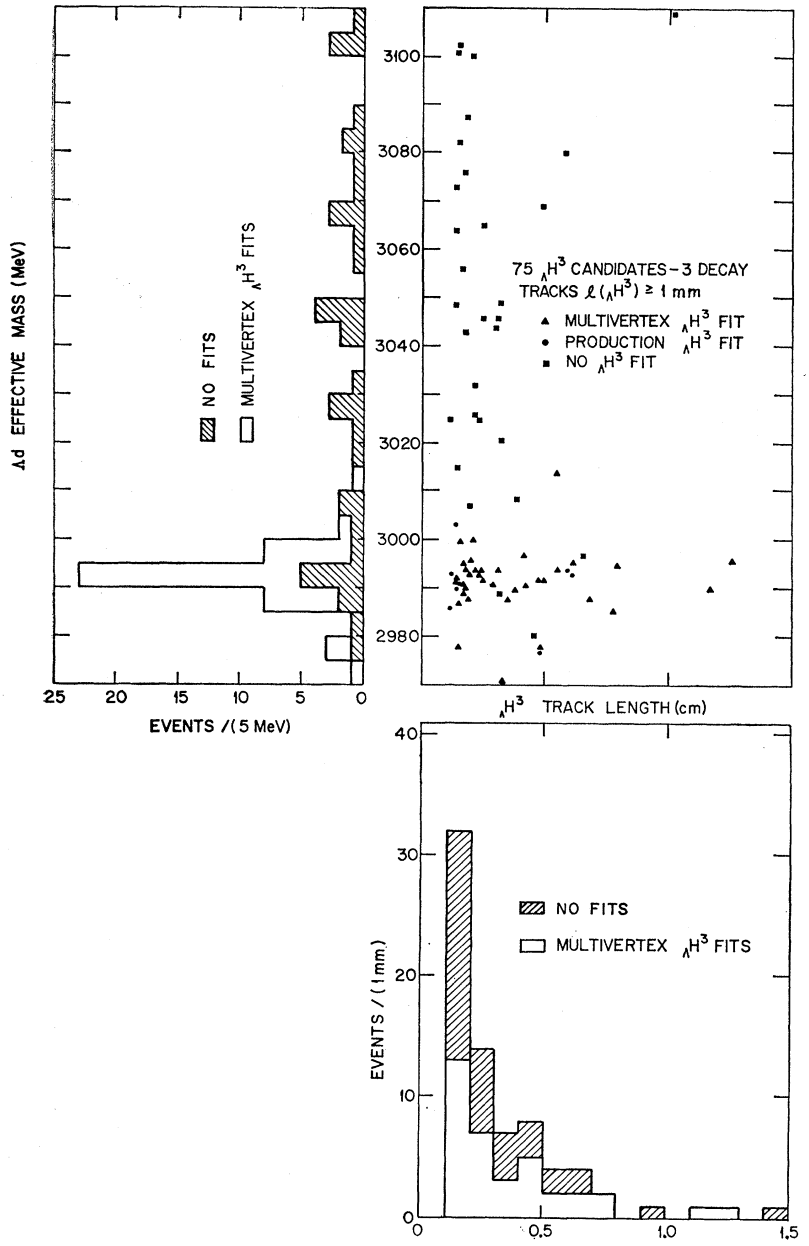

FIG. 7. Scatter plot of the missing mass from the production $p\pi^-$ system against the length of the ${}_\Lambda H^3$ track for all events selected by the editing physicist as candidates for the reaction $K^-+He^4 \rightarrow {}_\Lambda H^3+p+\pi^-$. All events have three charged tracks at the decay vertex. The mass was determined using production kinematics only.

are unambiguously identified by multivertex fits including both production and decay. The 65 multibody decays [reactions (1c) and (1d)] give a lifetime of $(1.34_{-0.16}{}^{+0.22})\times 10^{-10}$ sec, indicating that some systematic error is present in the data, or possibly that the two-body and the multibody decays come from a different spin state of the hypernucleus. The former possibility was found to be correct, as will be explained shortly. The latter possibility is unlikely since the spin-$\frac{3}{2}$ state, even if bound, is calculated to have a longer lifetime than the spin-$\frac{1}{2}$ state.[12] The spin-$\frac{3}{2}$ state should favor the multibody decay because of the dominance of the S wave in the Λ decay.

Several systematic checks were made on the data. The lifetime from events found on only one of two scans was consistent with that from events found on both scans. The mean ${}_\Lambda H^3$ track length for both samples was 5.7 mm. The two experimental groups found the same lifetime from the two-body decays and from the multibody decays as seen in Table II. Also, most of the events analyzed at Carnegie have been analyzed independently at Argonne. These checks revealed no significant differences in scanning or data reduction between the two groups.

[12] B. W. Downs and R. H. Dalitz, Phys. Rev. **114**, 593 (1959).

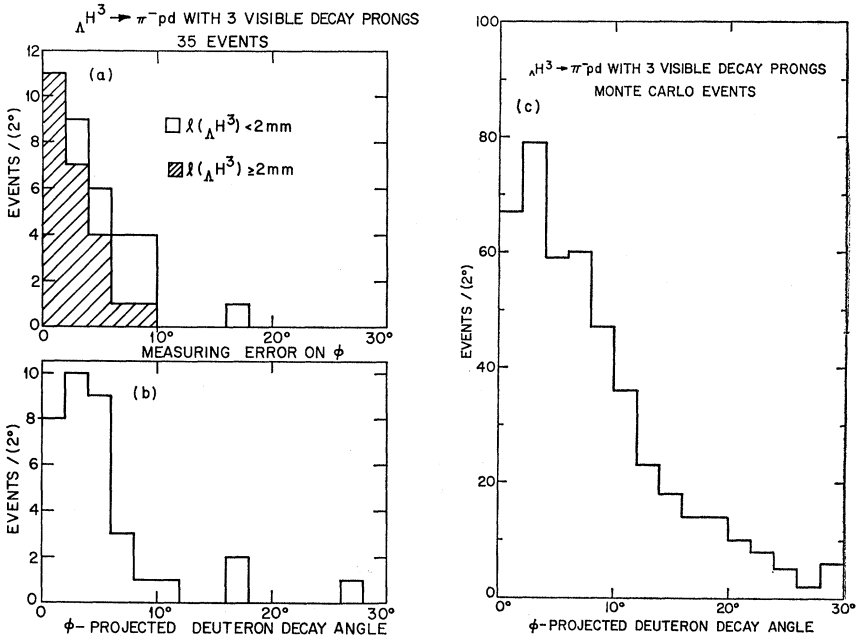

FIG. 8. (a) Measuring error on the projected angle of the decay deuteron in the laboratory system with respect to the line of flight of the $_{\Lambda}H^{3}$ for the three-body three-prong events of Table I. (b) Measured angle whose error is plotted in (a). (c) Expected deuteron decay angular distribution from a Monte Carlo calculation.

As an additional check on procedures, the lifetime of the Σ^{+} was obtained using events from the reaction

$$K^{-}+\mathrm{He}^{4} \rightarrow \Sigma^{+}+\pi^{-}+\mathrm{He}^{3}.$$

These events are topologically similar to $_{\Lambda}H^{3}$ events and thus serve as a strong test of the over-all procedures. The mean lifetime obtained from 86 events was $(0.84 \pm 0.13)\times 10^{-10}$ sec, compared to the world average of $(0.810\pm 0.013)\times 10^{-10}$ sec.[13]

The mean lifetime for the free Λ was also measured from a sample of 1293 events which gave multivertex fits to the final state $\Lambda\pi^{-}\mathrm{He}^{3}$. The best value from a maximum-likelihood analysis was $(2.58\pm 0.10)\times 10^{-10}$ sec compared to an expected $(2.52\pm 0.03)\times 10^{-10}$ sec.[13]

The lifetime was measured as a function of the $_{\Lambda}H^{3}$ decay cutoff momentum p_D, used to separate in-flight decays from at-rest decays, over the interval 0–300 MeV/c. The distribution of decay momenta indicates that, due to measurement errors, all hyperfragment momenta within 150 MeV/c of zero are consistent with decays at rest. If account is not taken of this error, the lifetime will be systematically underestimated due to misclassification of decays at rest as decays in flight. With $p_D=0$ MeV/c we found $\tau=(2.0_{-0.3}{}^{+0.4})\times 10^{-10}$ sec, while beyond 140 MeV/c the lifetime was flat as a function of p_D with $\tau=(2.5_{-0.4}{}^{+0.6})\times 10^{-10}$ sec. We choose $p_D=170$ MeV/c, corresponding to a hyperfragment residual range of 1 mm.

Figure 6 shows the sensitivity of the $_{\Lambda}H^{3}$ lifetime to minimum accepted $_{\Lambda}H^{3}$ track length. The two-body decays give consistent results over the interval $1 \leqslant l \leqslant 5$ mm. A scanning bias against short-length $_{\Lambda}H^{3}$ events would give a negative slope for this plot. Since the data for all lengths are consistent, we have chosen to quote the value at 1 mm for the two-body decays to keep the maximum number of events, and so obtain the value $\tau=(2.64_{-0.52}{}^{+0.84})\times 10^{-10}$ sec stated earlier.

The lifetime from three- and four-body decays as a function of the minimum accepted $_{\Lambda}H^{3}$ track length is shown in Fig. 6(b). Here one observes a noticeable positive slope to the data between 1 and 2.5 mm and even the Block result[4] at 0.5 mm is in accord with such a slope, in contrast to the result from the two-body decays shown in Fig. 6(a). The slope in this region seems to be a result of contamination from Λ overlay events, where a Λ from the final state $\Lambda\pi^{-}pd$ decays in spatial coincidence with the deuteron track and thus simulates a $_{\Lambda}H^{3}$ event. This problem is most severe at short hyperfragment track lengths and diminishes at longer distances from the production vertex. For example, the maximum transverse momentum which will yield an overlay at 1 mm is $\sim$150 MeV/c for a 300-MeV/c Λd system, while at 2.5 mm this becomes only 50–60 MeV/c.

Our kinematic discrimination is not sufficient to separate the bound $_{\Lambda}H^{3}$ events from the Λ overlay events on an individual event basis. A scatter diagram of the effective mass of the Λd system against the length of the decaying track for all $_{\Lambda}H^{3}$ candidates with three secondary prongs is shown on Fig. 7. All events which passed the editing criteria are included on this plot. The Λd mass projection for events with $_{\Lambda}H^{3}$ track length $\geqslant 1$ mm indicates that the mass resolution at the primary vertex is about ± 5 MeV. The cross-hatched squares represent Λ overlays that do not fit the $_{\Lambda}H^{3}$ hypothesis. The open squares represent events which

[13] Particle Data Group, Rev. Mod. Phys. 41, 109 (1969).

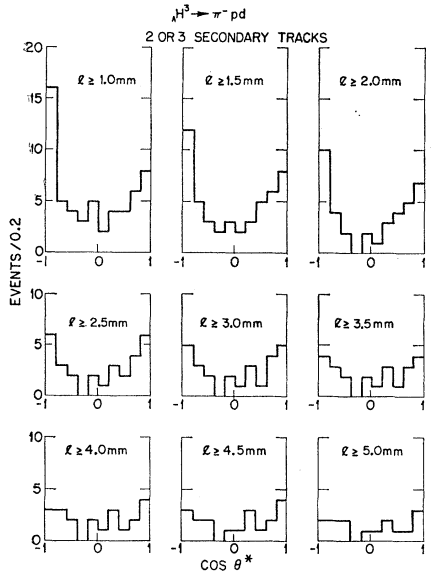

FIG. 9. Angular distribution of the decay deuteron in the $_\Lambda H^3$ rest frame with respect to the $_\Lambda H^3$ line of flight for all three-body decay events. The minimum accepted $_\Lambda H^3$ track length is indicated on each histogram. The enhancements in forward and backward directions are caused by Λ overlay contamination, since the distribution should be isotropic for the decay of a spin-$\frac{1}{2}$ $_\Lambda H^3$.

have acceptable fits to the $_\Lambda H^3$ hypothesis. There are some $\Lambda\pi^- pd$ events in the $_\Lambda H^3$ mass region that are unambiguous because of the transverse momentum of the Λ or the range-energy resolution on the connecting track. However, all except two of the un-cross-hatched events also fit the $\Lambda\pi^- pd$ hypothesis with a probability comparable to that for the $_\Lambda H^3$ fit. The kinematic fitting procedure therefore provides little separation of real $_\Lambda H^3$ events from Λ overlays. The overlay problem is potentially serious because 11% of all K^- stops yield the final state $\Lambda\pi^- pd$, whereas the hypertriton production is only $\sim$0.2% of K^- stops.

One might expect that this background could be minimized by a careful study of the angle between the deuteron track from the decay and the $_\Lambda H^3$ track. Some information can be obtained from this technique, as is illustrated by Fig. 8, which shows this decay angle and its error. Also shown is a Monte Carlo histogram where we have input our best knowledge of errors and have used our production momentum distribution for $_\Lambda H^3$ and the deuteron momentum distribution from the European emulsion collaboration.[14] We see that with our resolution, about 75% of the real events are consistent with a zero decay angle; searching for decay angles inconsistent with zero is then an inefficient way of separating real events from background.

This background is seen more dramatically on Fig. 9, which shows the angular distribution of the decay deuteron in the $_\Lambda H^3$ rest frame with respect to the line of flight of the hypertriton. This distribution should be isotropic for the decay of a spin-$\frac{1}{2}$ $_\Lambda H^3$. We see that at $l \gtrsim 1$ mm there is a definite enhancement in the forward and backward directions, for events with short "hyperfragment" tracks. This figure indicates that we do not have a pure sample of $_\Lambda H^3$ events with a cut at $l \lesssim 4$ mm.

We can estimate the contamination in the three-body decays by assuming that the sample with $l \gtrsim 4$ mm is pure and asking how many true events should be observed with $l \gtrsim 1$ mm. Assuming a lifetime of 2.4×10^{-10} sec, this procedure gives 39 ± 9 expected events, compared to 57 observed, a contamination of 18 ± 9 events.

The estimated pure component corresponds to a uniform distribution in the plot at a level of about four events per bin. This level of background is consistent with Monte Carlo results which use the observed unambiguous $\Lambda\pi^- pd$ events to estimate the number of Λ overlays.

The most reliable lifetime from this experiment is from the two-body decay events. The background studies in the three-body decay mode indicate that a reasonably pure sample of $_\Lambda H^3$ can be obtained by using only those events with $l(_\Lambda H^3) \gtrsim 4$ mm. Since this doubles the number of events, we mention the result from those events with the understanding that some contamination may remain in the sample. The lifetime from the multibody decays with $l \gtrsim 4$ mm is $\tau = (1.93_{-0.37}{}^{+0.60})\times10^{-10}$ sec based on 27 events. Combining these with the 27 two-body decay events having $l \gtrsim 1$ mm, we obtain an over-all lifetime of $\tau = (2.28_{-0.33}{}^{+0.46})\times10^{-10}$ sec from 35 decays in flight and 19 decays at rest. Since any residual background of Λ overlays will only lower the lifetime, the combined result can be considered a reliable lower limit.

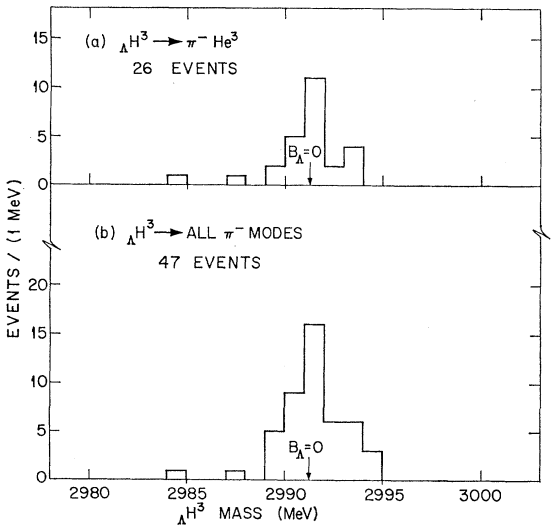

FIG. 10. $_\Lambda H^3$ mass distribution for events which decay into (a) the two-body final state π^- He^3 with $l(_\Lambda H^3) \gtrsim 1$ mm, (b) multibody final states $\pi^- pd$ and $\pi^- ppn$ with $l(_\Lambda H^3) \gtrsim 4$ mm combined with the two-body events of (a). Kinematic information from both the production and decay vertices has been used. The arrow indicates zero binding using the Λ mass determined from this experiment.

[14] J. Sacton (private communication).

TABLE III. $_{\Lambda}H^{3}$ lifetime results.

$_{\Lambda}H^{3}$ mean life (10^{-10} sec)	Technique	Reference
$2.64_{-0.52}^{+0.84}$	Helium bubble chamber	This experiment; two-body decays
$2.28_{-0.33}^{+0.46}$	Helium bubble chamber	This experiment; lower limit from two- and three-body decays
$0.95_{-0.15}^{+0.19}$	Helium bubble chamber	Block *et al.* (Ref. 4)
$2.85_{-1.05}^{+1.27}$	Nuclear emulsion	Phillips and Schneps (Ref. 15)
$1.28_{-0.26}^{+0.35}$	Nuclear emulsion	Bohm *et al.* (Ref. 16)
2.39 ± 0.12	Calculation for $J=\frac{1}{2}$	Rayet and Dalitz (Ref. 17)[a]
3.15 ± 0.65	Calculation for $J=\frac{3}{2}$	Dalitz and Rajasekharan (Ref. 18)[a]

[a] The numerical integrals involved in these calculations have been re-evaluated using a more recent value for the mean pion momentum for the multibody decays (see Ref. 4).

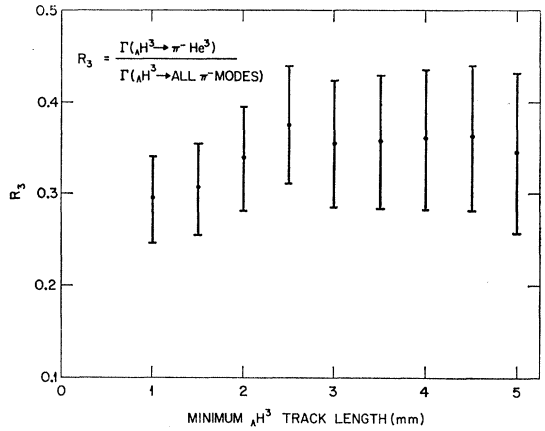

FIG. 12. Two-body mesonic decay branching ratio R_3 for $_{\Lambda}H^{3}$ as a function of the minimum accepted $_{\Lambda}H^{3}$ track length.

Possible systematic errors coming from uncertainties in the range-energy relation, magnetic field, distance measurements in the chamber, or $_{\Lambda}H^{3}$ mass were all found to be negligible.

Table III summarizes the present results and previously reported measurements of the lifetime and also the theoretical predictions for hypernuclear spins of $\frac{1}{2}$ and $\frac{3}{2}$.[15–18] In nuclear emulsions it is not always possible to distinguish the $_{\Lambda}H^{3}$ events from $_{\Lambda}H^{4}$. There is also the possibility that the very weakly bound $_{\Lambda}H^{3}$ will suffer Coulomb disintegration to a Λ and a deuteron while in flight in the nuclear emulsion. Estimates of the cross section for this process[19] put it in the range of tens of barns, which could seriously lower the lifetime as measured in emulsion.

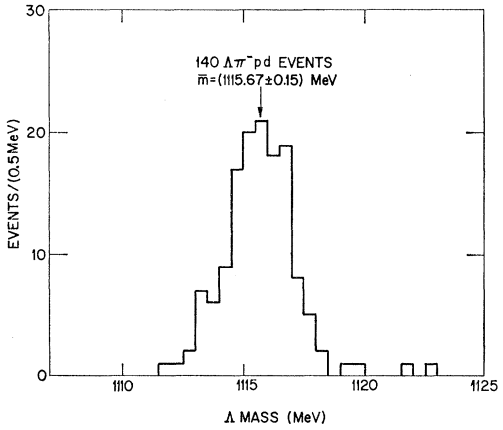

FIG. 11. Λ mass distribution from 140 events which have multi-vertex fits to the hypothesis $\Lambda\pi^-pd$ with χ^2 probability $\geq 1\%$.

[15] R. E. Phillips and J. Schneps, Phys. Rev. Letters **20**, 1383 (1968).
[16] European K^- collaboration (to be published).
[17] M. Rayet and R. H. Dalitz, Nuovo Cimento **46A**, 786 (1966).
[18] R. H. Dalitz and G. Rajasekharan, Phys. Letters **1**, 58 (1962).
[19] N. N. Kolesnikov and R. V. Vedrinsky, Nuovo Cimento **43B**, 301 (1966).

Neither of these problems exists in a helium bubble chamber. The present result should be more reliable than the earlier helium-chamber measurement in that about twice as many events are involved, the chamber is larger so that escape corrections are negligible, and the momentum precision is very much better because of the 3-times-higher magnetic field. The momentum precision is an essential factor in eliminating various kinds of background events. Techniques have also improved in recent years, particularly in kinematic fitting programs.

B. Binding Energy and Decay Branching Ratio

We have determined the binding energy of $_{\Lambda}H^{3}$ by a direct measurement, which consists of kinematically fitting all events for various values of the $_{\Lambda}H^{3}$ mass and observing the χ^2 goodness of fit. The best mass and error were taken to correspond to the minimum χ^2 and a change of 1.0 from the minimum value. Errors thus determined agree with the width of the mass distribution from all events. The several measurements of each event were then combined using the measuring errors as weighting factors to give a best mass for each event. The results for all two- and three-body decay events are shown separately and combined on Fig. 10. The mass values are 2991.00 ± 0.27 MeV for the 26 two-body decays and 2992.19 ± 0.22 MeV for the 58 three-body decays using the events from Table I with $l(_{\Lambda}H^{3}) \geq 1$ mm. The difference, of over 3 standard deviations, is consistent with the three-body decays being contaminated with Λ overlays as before, which here increase the apparent mass of the $_{\Lambda}H^{3}$. The three-body decays with $l \geq 4$ mm give a mass of 2991.99 ± 0.40 MeV and, when these are combined with the 26 two-body decays, the over-all result is 2991.32 ± 0.22 MeV.

We have measured the mass of the free Λ in the same manner from a sample of 140 events with visible $\Lambda\pi^-pd$ in the final state. The mass distribution is shown on Fig. 11. The best value from a weighted mean is 1115.67

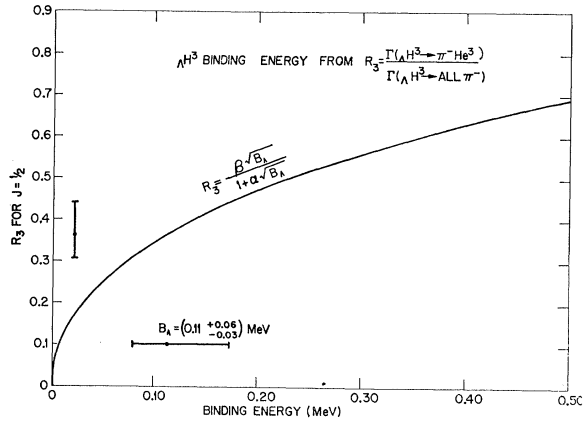

FIG. 13. Theoretical relation between the decay branching ratio R_3 and the $_\Lambda H^3$ binding energy for $J(_\Lambda H^3)=\frac{1}{2}$. Numerical integrals from Ref. 23 have been used. The result from this experiment is shown.

± 0.15 MeV, which agrees with the world average 1115.60 ± 0.08 MeV.[13]

The binding energy of the Λ to the deuteron core is calculated using our Λ-mass result and 1875.582 MeV for the deuteron mass. The two-body decay events give $B_\Lambda=0.25\pm 0.31$ MeV, while the combined decays give $B_\Lambda=-0.07\pm 0.27$ MeV. These results should be compared to the two emulsion measurements 0.06 ± 0.06 [20] and 0.24 ± 0.12 MeV.[21]

The decay branching ratio R_3 defined as

$$R_3=\Gamma(_\Lambda H^3\to \pi^- He^3)/\Gamma(_\Lambda H^3\to \text{all } \pi^- \text{ modes})$$

is important because of its sensitivity to the spin of $_\Lambda H^3$. It can also be used to obtain an indirect measurement of the binding energy[22] according to the equation

$$R_3=\frac{\beta\sqrt{B_\Lambda}}{1+\alpha\sqrt{B_\Lambda}}.$$

With Leon's[23] evaluation of the integrals at $B_\Lambda=0.25$ MeV, the constants are $\beta=1.22$ and $\alpha=0.21$.

Our values of R_3 are shown on Fig. 12 as a function of the minimum accepted $_\Lambda H^3$ track length. The background contamination with $1\leqslant l\leqslant 3$ mm is apparent. We maximize the statistics as previously described by using all two-body decays with $l\geqslant 1$ mm and estimating the number of three-body decays at $l\geqslant 1$ mm from the events with $l\geqslant 4$ mm. This yields $R_3=0.36_{-0.06}{}^{+0.08}$, where we have included the effect of a 25% underestimate of the background in the upper error. This

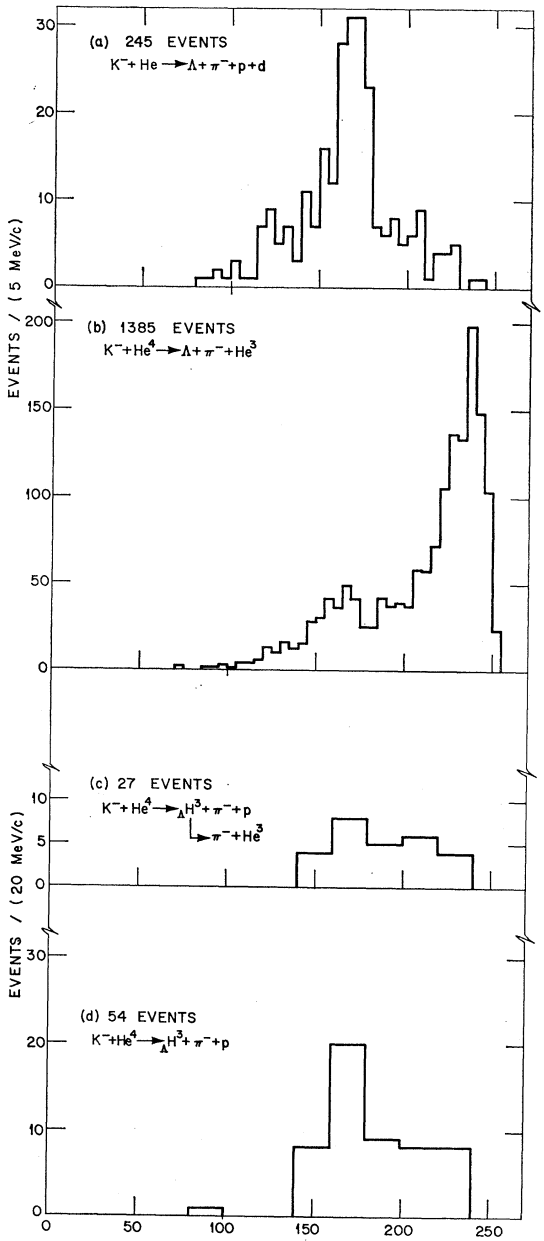

FIG. 14. Momentum distributions of the π^- produced by K^- interactions at rest in He^4 resulting in the final states shown. The enhancement at $\sim$170 MeV/c in (a) results from the two-step process of Σ production followed by Σ/Λ conversion within the nucleus. In (b), the dominant contribution is direct Λ production with a He^3 spectator, $K^-n(He^3)\to\Lambda\pi^-(He^3)$. The $_\Lambda H^3$ events with $l(_\Lambda H^3)\geqslant 1$ mm which decay into the two-body mode π^-He^3 are shown on (c), and these are combined with the multibody decay mode events with $l(_\Lambda H^3)\geqslant 4$ mm in (d).

[20] G. Bohm, J. Klabuhn, U. Krecker, F. Wysotski, G. Coremans, W. Gajewski, C. Mayeur, J. Sacton, P. Vilain, G. Wilquet, D. O'Sullivan, D. Stanley, D. H. Davis, E. R. Fletcher, S. P. Lovell, N. C. Roy, J. H. Wickens, A. Filipkowski, K. Garbowska-Pniewska, T. Pniewska, E. Skrzypczak, T. Sobczak, J. E. Allen, V. A. Bull, A. P. Conway, A. Fishwick, and P. V. March, Nucl. Phys. **B4**, 511 (1968).

[21] K. N. Chaudhari, S. N. Ganguli, N. K. Rao, M. S. Swami, A. Gurtu, J. M. Kohli, and M. B. Singh, TIFR Report No. NE-68-8, 1968 (unpublished).

[22] M. M. Block, R. Gessaroli, J. Kopelman, S. Ratti, M. Schneeberger, L. Grimellini, T. Kikuchi, L. Lendinara, L. Monari, W. Becker, and E. Harth, in *Proceedings of the International Conference on Hyperfragments, St. Cergue, 1963* (CERN, Geneva, 1964).

[23] M. Leon, Phys. Rev. **113**, 1604 (1959).

value agrees with the emulsion results $0.39_{-0.07}^{+0.12}$ [24] and 0.43–0.48±0.04,[25] and with the previous helium-bubble-chamber result of 0.39±0.07,[22] although this latter agreement may be fortuitous.

These values of R_3, together with the determination of the s/p ratio for the free Λ decay, determine the spin of $_{\Lambda}H^3$ to be $\frac{1}{2}$.[1] Figure 13 shows the relation between R_3 and B_Λ which gives the result $B_\Lambda=0.11_{-0.03}^{+0.06}$ MeV, in good agreement with the direct measurements.

C. Production Kinematics and Rate

Figure 14 shows the momentum spectrum of the production pion for the $_{\Lambda}H^3$ events and for events of the final states $\Lambda\pi^- pd$ and $\Lambda\pi^-He^3$.[26] The latter is dominated by the impulse peak coming from the pseudo-two-body reaction $K^-n\rightarrow\Lambda\pi^-$, with a He^3 spectator. Events where the He^3 breaks up to $p+d$ arise mainly from a Σ-Λ conversion process in which a Σ hyperon is initially produced by the reaction $K^-N\rightarrow\Sigma\pi^-$ followed by the conversion $\Sigma+N\rightarrow\Lambda+N$. The pion momentum spectrum for the hypertriton events is qualitatively similar to that for the $\pi^-\Lambda pd$ final state, which suggests that the hyperfragment formation may also involve Σ-Λ conversion. This kind of effect is also seen in hyperfragment production by K^- interactions in nuclear emulsion.[27]

The production rate for the reaction

$$K^-+He^4\rightarrow{}_{\Lambda}H^3+\pi^-+p$$

was measured in this experiment to be $(1.8_{-0.06}^{+0.07})\times10^{-3}$ per stopping K^-. The number of stopping kaons was determined[28] by counting the K^- interactions every 20 frames. To determine the number of these interactions that occurred at rest, the K^- track for 1000 of these interactions was measured. The momentum at the interaction point was determined by reducing the momentum measured by the curvature at the track midpoint by the energy loss determined from the range of the track.

The partial rate for the π^- decay mode, which is the only observed decay, is $(1.2\pm0.4)\times10^{-3}$ per stopping K^- based on the observation of the 27 two-body decay events and 48_{-9}^{+14} three-body decay events. The rate for two-body decays alone is $(0.42\pm0.12)\times10^{-3}$ per K^- stop. Corrections to the observed events include a 12% scanning-efficiency correction, a solid-angle correction of 9%, a hyperfragment-length correction of 17% for events shorter than 1 mm, and a correction of 5% for unmeasurable events. The quoted over-all $_{\Lambda}H^3$ rate includes corrections of 53% for π^0 decays[29] and 1.3% for nonmesonic decays.[17]

VIII. CONCLUSIONS

The hypertriton was studied using a helium bubble chamber and a stopping K^- beam. The mean life of the hypertriton was measured to be $(2.64_{-0.52}^{+0.84})\times10^{-10}$ sec using 27 two-body decay events only. The result agrees well with theoretical expectation and disagrees with the previous helium-bubble-chamber measurement. A serious source of background was found in the multibody decays. After appropriate cuts, the 27 remaining multibody decays gave a lifetime of $(1.93_{-0.37}^{+0.06})\times10^{-10}$ sec, in agreement with the value obtained from the two-body decays. The combined result of $(2.28_{-0.33}^{+0.46})\times10^{-10}$ sec should be a reliable lower limit.

The production rate for the reaction $K^-He^4\rightarrow{}_{\Lambda}H^3p\pi^-$ was measured to be $(1.8_{-0.6}^{+0.7})\times10^{-3}$ per stopping K^-. Our measurement of the binding energy which uses mostly curvature information agrees with previous emulsion determinations which use range measurements. The ratio R_3 of the two-body π^- decay (π^-He^3) to all π^- decay modes also agrees with previous measurements and so confirms the spin of $_{\Lambda}H^3$ to be $\frac{1}{2}$.

ACKNOWLEDGMENTS

We wish to thank the ZGS operations group and the technical staff of the bubble chamber for making this experiment possible. Excellent service was given by Hope Chaffee, Modesta Umbrasas, Chris Dedin, and Joyce Brandalino, who scanned the film at Argonne. The Carnegie group wish to acknowledge the help of Joe Rudman, who directed the scanning effort there.

[24] R. G. Ammar, W. Dunn, and M. Holland, Nuovo Cimento **26**, 840 (1962).
[25] D. H. Davis and J. Sacton, in Proceedings of the International Hypernuclear Conference, Argonne National Laboratory, 1969, p. 159 (unpublished).
[26] K. Burnell, Ph.D. thesis (unpublished).
[27] J. W. Patrick and P. L. Jain, Nucl. Phys. **73**, 681 (1965).
[28] A detailed discussion of this point can be found in P. Katz, K. Bunnell, M. Derrick, T. Fields, L. G. Hyman, and G. Keyes, Phys. Rev. (to be published).
[29] R. H. Dalitz and L. Liu, Phys. Rev. **116**, 1312 (1959).